



Improved source assessment of Si, Al and related mineral components to PM₁₀ based on a daily sampling procedure

Ge Peng^{1,2,*}, Hans Puxbaum², Heidi Bauer², Nicole Jankowski², Yao Shi³

1. Chemical Engineering College, Ningbo University of Technology, Ningbo 315016, China. E-mail: gepengv@hotmail.com

2. Institute for Chemical Technologies and Analytics, Vienna University of Technology, Vienna 1060, Austria

3. College of Environmental and Resource Sciences, Zhejiang University, Hangzhou 310027, China

Received 24 June 2009; revised 23 August 2009; accepted 31 August 2009

Abstract

Samples obtained from an industrialized valley in the East Alpine region were collected daily for a half year and analyzed using X-ray fluorescence to examine the elements Si, Al, Fe, Ca, Mg, Na, K, Zn, P, S and Cl. Some factors affecting the changes of these elements were considered, including time, elemental correlations, weekday, weekend and seasonal changes. Diagnostic analysis provided an insight into a decoupling behavior that occurs in siliceous and carbonates minerals. A decrease in Si and Al and an increase in carbonates, Na, K, Zn and P were observed during the cold season. However, a consistently high correlation of Si and Al was observed in all seasons. It was established that such high levels originated from street surface abrasion. The increase in variability and absolute levels of carbonates during the cold season was demonstrated by adding carbonates to the street surface as gritting material to increase the grip on snowy surfaces. A marked increase in Na and Cl was observed in winter which may have been caused by thaw salt that is widely used in winter in Austria. This was associated with a significant increase in K, Zn, and P in the cold season that was the result of domestic space heating with wood. PM₁₀ levels in December were 12 µg/m³ and were higher than levels detected in July. It was established that such high levels originated from mineral oxides, wood smoke, and inorganic ionic material(s).

Key words: particulate matter PM₁₀; mineral aerosol; silicates; carbonates; street dust; wood combustion; thaw salt

DOI: 10.1016/S1001-0742(09)60149-2

Introduction

The main constituents of “fine” atmospheric aerosol particles (PM_{2.5}) are inorganic secondary constituents and carbonaceous material. However, “coarse” particulate matter (PM_{2.5–10}) generally contains “mineral” constituents such as silicates and carbonates (Querol et al., 2004; Viana et al., 2008). Elements of interest in the “mineral” fraction had elevated concentrations of Si, Al, Fe, Ca, Mg, Na, K, Cl, and S, while trace elements, typically P, Ti, Ba, Cu, Mn and Zn, were present at levels of 0.05%–0.5% in ambient air samples (Maenhaut and Cafmeyer, 1998).

Most silicates are poorly soluble in acid and are difficult to analyze using conventional techniques such as atomic absorption spectrometry (AAS) and inductively coupled plasma (ICP) analysis. However neutron activation analysis (NAA) X-ray fluorescence (XRF) techniques are commonly used in their analysis (Merian et al., 2004). Additionally, XRF techniques have also been used to determinate Si and Al in atmospheric particulate matter (Gilfrich et al., 1973; Hammerle and Pierson, 1975) by using glass and quartz fiber filters for PM sampling of organic constituents, ions and trace metals in air (Rogge

et al., 1993; Puteaud et al., 2004). Filters energy dispersive (EDS) and wavelength dispersive (WLD) XRF techniques have also been used in direct determination of mineral elements (Wang et al., 1996; Marcazzan et al., 2004). However, it has been demonstrated that WLD-XRF exhibits a better resolution than that EDS-XRF since it is capable of determining major and minor elements of the atmospheric aerosol, including those components that are difficult to determine with other techniques (Watson et al., 1999).

The literature also demonstrates that other techniques such as total reflection XRF (Leland et al., 1987); proton induced XRF or synchrotron XRF (Bukowiecki et al., 2005) can also be used in the analysis of PM, however, such methods require special instrumentation that are not commonplace in most laboratories. In this article, the research focussed on the use of a WLD-XRF method in the determination of Si, Al, Fe, Ca, Mg, Na, K, Ba, Cu, Zn, Cl, S and P in atmospheric PM samples (ambient and source air) that were collected on 47 mm mixed cellulose ester filters. The results indicated that the method was a useful analytical technique that compared favourably with ICP-OES. Furthermore, results indicated that it was possible to discriminate between specific winter sources such as wood combustion, thaw salt, gritting material and their contribution to atmospheric PM₁₀ levels by extending the

* Corresponding author. E-mail: gepengv@hotmail.com

resolution time to 24 hr. This technique was therefore used in the comparison of specific winter and summer sources of PM.

1 Experimental

1.1 PM₁₀ emission and ambient samples

Source samples of “street dust” were collected by sweeping side pavements of streets in Vienna, Austria. The PM₁₀ fraction from samples was isolated using a manifold where the dust was resuspended and the PM₁₀ fraction was collected onto a low volume filter (Gelman Metrical GN-4) with a PM₁₀ inlet (Digital DPM₁₀ inlet for a flow rate of 1 m³/hr, active sampling diameter of 40 mm equivalent to a surface area of 1257 mm²).

Ambient samples were collected from air quality measurement sites of Styria, Austria. The samples were collected daily (0–24 hr) at two adjacent sites in the city of Leoben (Goess 554 m; 15°06′17″E, 47°21′34″N; and Donawitz 555 m, 15°04′28″E, 47°22′33″N), where is an industrialized valley (Murtal) with 24,000 inhabitants. A LECKEL SEQ 47/50 sampler with PM₁₀ size selective inlets LVS3 with a sampling rate of 2.3 m³/hr was used to collect samples. The filter (Gelman Metrical GN-4) has an active sampling diameter of 38.4 mm, equivalent to an area of 1158 mm². The study focussed on the Goess data set while the Donawitz data set served to check the validity of the assumptions made in the Goess data set. Simultaneously sampling was performed on 150 mm diameter of Pallflex QAT-UP 2500 Quartz fiber filters with DIGITEL DA80H Hi with PM₁₀ inlet for a flow rate of 30 m³/hr. Following filtration PM₁₀ mass, ions, carbon parameters and selected organic compounds were then determined. Sampling was performed daily over a time period of 6 months (July–December, 2006) period including summer and winter months.

1.2 Analytical methods

1.2.1 Weighing and sample preparation

Gravimetric analysis was performed using a microbalance (Sartorius Micro MC210P, sensitivity 1 µg) after samples were equilibrated for 48 hours at (20 ± 1)°C and a relative humidity of (50 ± 5)% according to the European standard method EN12341. In the XRF technique the whole Gelman Metrical GN-4 filter was used to collect the samples. For the analysis of ions and carbonaceous components small discs (10 and 12 mm Ø discs) were punched from the filters using steel punches. Trace metal analyses were conducted using 10 mm Ø disks that were also prepared daily using a home-made glass punch.

1.2.2 XRF method

XRF analysis was performed using a Philips 1480 wavelength-dispersive X-ray fluorescence spectrometer, fitted with a rhodium target X-ray tube ($K_{\alpha} = 0.616 \text{ \AA}$). The tube was set at 50 kV with a current of 40 mA, and time for counting on analytical line and background are 20, and 10 sec, respectively.

A flow proportional detector (operated with a 10% (V/V) methane in argon PR-gas) was used for the detection of Ba in elemental analyses (Messer-Griesheim, Gumpoldskirchen). Ba was then quantified by using a scintillation counter.

Filter samples were introduced in a holder with a central opening of 27 mm diameter. The sample holder was then placed into an inlet, where the sample was automatically transferred into the analytical chamber using a vacuum of < 10 Pa. The X-ray beam was 24 mm in diameter and was directed on to the centre of the filter holder. The parameters used in XRF analyses of the major elements (Si, Al, K, Na, Ca, Mg, Cl, S, and trace Zn, Cu, Fe, P and Ba) are listed in Table 1.

Table 1 Instrumental parameters for the XRF determination

Line	λ (Å)	Crystal	Number of background measurements
Si K_{α}	7.124	PE002	2
Al K_{α}	8.3401	PE002	1
K K_{α}	3.741	LIF200	1
Na K_{α}	11.908	TLAP	1
Ca K_{α}	3.359	LIF200	2
Mg K_{α}	9.888	TLAP	1
Cl K_{α}	4.728	GE111	2
S K_{α}	5.371	GE111	2
Zn K_{α}	1.435	LIF200	2
Cu K_{α}	1.542	LIF200	2
Fe K_{α}	1.935	LIF200	2
P K_{α}	6.158	GE111	1
Ba K_{α}	0.385	LIF200	2

Line: analytical line; λ : wavelength; crystal: analyzed crystal.

1.2.3 Calibration

Several calibration standards were used, including a powdered mineral standard. Powdered certified standard samples (Soil: San Joaquin soil from National Institute of Standards, USA, NIST SRM 2709; and Bush: Bush Branches and Leaves from China National Analysis Center for Iron and Steel, NCS DC73349), and a particulate filter standard (NIST air particulate on filter media SRM2783) were sorbed to filter disks and were used as quality control. The chemical compositions of standards and samples (collected from the crustal composition, street dust and ambient particulates PM₁₀ samples from a Vienna site) are compared in Table 2.

Filter blanks were determined using 20 samples from 4 different calibration runs. Detection limits (DL), derived from 3 SD of the blanks were transformed to mg/filter and air equivalents as listed in Table 3. Detection limits were in the range of 0.4 (for P)–18.5 (for Ca) ng/m³ and used for analytes. The elevated DL for Ca resulted from a notable Ca concentrations in the blank filters.

1.2.4 Calibration curves

Calibration was performed using filters containing PM₁₀ fractions of the standards (Soil and Bush). For each standard, 3 to 5 filter samples with loadings in the range of 0.3 to 30.0 mg PM₁₀ fraction were prepared. Concentrations of the individual elements are listed in Table 4. The upper

Table 2 Chemical composition of standard samples and comparison with the crustal composition, street dust and urban particulate matter

	Soil (m)	Bush (m)	Crust W95 ^a (m)	Street dust Vienna ^b (m)	Vienna RBS ^c (m)
Si	29.7	0.60	28.8	20.60	6.37
Al	7.50	0.20	7.96	5.48	1.76
K	2.03	0.92	2.14	0.090	0.54
Na	1.16	1.96	2.36	0.060	1.01
Ca	1.89	1.68	3.85	14.68	3.70
Mg	1.51	0.48	2.2	2.28	0.75
Cl	n.r.	1.92	0.047	0.130	1.00
S	0.089	0.73	0.07	0.061	4.00
Zn	0.011	0.0055	0.0065	0.110	0.14
Cu	0.004	0.0007	0.0025	0.017	0.061
Fe	3.50	0.107	4.32	2.44	2.23
P	0.062	0.10	0.076	n.r.	n.r.
Ba	0.097	0.0018	0.058	0.040	0.036

^a Average for upper crust composition according to Wedepohl (1995).^b Average concentration from street dust samples from sites in Vienna (N. Jankowski, unpublished data).^c Annual average 2004 from a traffic site (Rinnböckstraße) in Vienna (Bauer et al., 2007; AQUELLA report Vienna).

Vienna RBS: traffic site “Rinnboeckstrasse”; n.r.: not reported

Table 3 Analytical results for filter blanks and derived standard deviation (SD), 3SD and detection limit (DL)

	Ave (kcps)	SD blank (mg/filter)	3SD (mg/filter)	DL (mg/filter)	DL ($\mu\text{g}/\text{m}^3$)
Si	0.0040	0.0008	0.0024	0.00016	0.0029
Al	0.0054	0.0007	0.0021	0.00008	0.0015
K	0.0022	0.0007	0.0020	0.00032	0.0058
Na	0.0004	0.0004	0.0011	0.00063	0.0114
Ca	0.0602	0.0024	0.0072	0.00102	0.0185
Mg	0.0014	0.0012	0.0037	0.00030	0.0055
Cl	0.0101	0.0017	0.0052	0.00032	0.0058
S	0.0286	0.0034	0.0102	0.00017	0.0031
Zn	0.0023	0.0007	0.0021	0.00017	0.0032
Fe	0.0358	0.0020	0.0060	0.00040	0.0072
P	0.0010	0.0005	0.0015	0.00002	0.0004
Ba	0.0017	0.0012	0.0037	0.0003	0.0054
Cu	0.0251	0.0019	0.0058	0.0005	0.0090

Ave: the average value for repeating 5 times.

limit for loading was 4 mg for the standard since higher loadings in sample loadings did not adhere adequately to filter surfaces. Further assessment of the quality of the calibration was performed by comparing data with that

obtained from a standard ambient filter sample (NIST air particulate on filter media SRM2783; as a certified standard).

Based on the limitations of the loading (−0.5 to 4.0 mg standard/filter) and the elemental content of the standards (Table 2), the working ranges of the method used for the individual elements were derived from the limits of quantification (2 times of the detection limits in Table 3) to the maximum loadings in the calibration runs times 1.5 (Table 4). Calibration functions for “Soil” samples resulted in linear or near linear response within the working ranges listed in Table 4.

2 Results and discussion

2.1 Results for ambient PM₁₀ samples from Goess

Time series of daily samples were collected from two adjacent sites in an industrialized valley of Styria. The series were analyzed for their daily, monthly and half-yearly averages. Analysis was performed at weekday-weekend days, warm and cold seasons. Table 5 lists the averages of the mineral elements for the half-year period, the EC (elemental carbon) and OC (organic carbon) content, and the particulate matter PM₁₀ mass concentrations.

The crystal elements Si and Al appeared to be closely coupled and decreased from the warm (July, August, September) to the cold season (November, December). It can be seen that the coupling was a high correlation between Si and Al with $R^2 = 0.835$ (Fig. 1). However, R^2 increased to 0.951 after removal of three outliers in the Al data. Two of the outliers occurred during the days of New Year Eve (Dec 31, Jan 1), which was originated from fireworks, while the third outlier was observed on Oct 30, 2006. Siliceous material in a smaller urban settlement may result from street abrasion, suspension or resuspension, agricultural activities, natural weathering and sporadic long range events of desert dust transport (Puteaud et al., 2004; Viana et al., 2008). On the basis of our observations, the sites in Austria street abrasion and mobilised soil dust are likely to be the major candidates for the occurrence of Si and Al (Limbeck et al., 2009). It is hypothesized,

Table 4 Amounts of analyte elements on individual standard filters from “Soil” (San Joaquin Soil NIST SRM 2709) and “working ranges”

	NIST 2783 ^a (mg/filter)	Soil NIST 2709 (mg/filter)					Working range (mg/filter)
Standard	–	0.69	1.31	1.48	1.67	2.34	
Si	0.0586	0.205	0.389	0.440	0.496	0.695	0.00032–1.1
Al	0.0232	0.052	0.098	0.111	0.125	0.176	0.00016–0.26
K	0.0053	0.014	0.027	0.030	0.034	0.048	0.00064–0.07
Na	0.0019	0.008	0.015	0.017	0.019	0.027	0.0013–0.04
Ca	0.0166	0.013	0.025	0.028	0.032	0.044	0.00204–0.07
Mg	0.0086	0.010	0.020	0.022	0.025	0.035	0.0006–0.05
Cl	n.r.	–	–	–	–	–	0.00032*
S	0.0011	0.0006	0.0012	0.0013	0.0015	0.0021	0.00034–0.003
Zn	0.0018	0.0007	0.00014	0.00016	0.00018	0.00025	0.00034–0.003 ^b
Cu	0.0005	0.00002	0.00005	0.00005	0.00006	0.00008	0.0005–0.0008 ^b
Fe	0.0265	0.0242	0.0459	0.0518	0.0585	0.0819	0.0008–0.1 ^a
P	n.r.	0.00043	0.00081	0.00092	0.00104	0.00145	0.00004–0.002
Ba	0.0003	0.0007	0.0013	0.0014	0.0016	0.0023	0.0003–0.003

Cl not certified in the soil standard; active filter area 12.6 cm².^a Defined filter area for 12.6 cm²; ^b upper working range defined from SRM2783; “–”: empty; *: no upper data available.

Table 5 Average results for ambient PM₁₀ samples from Goess (Styria, Austria) July 7, 2006–Jan 2, 2007

	Si	Al	Fe	Ca	Mg	Na	K	Zn	P	S	Cl	EC*	OC*	PM ₁₀	Al/Si	Ca/Si
Average																
(% in PM ₁₀)	1.78	0.48	1.92	1.18	0.49	2.59	3.07	0.24	0.25	2.81	1.16	–	–	–	–	–
(μg/m ³)	0.42	0.11	0.45	0.28	0.11	0.61	0.72	0.06	0.06	0.66	0.27	–	–	23.4	0.27	0.66
RSD (%)	65	71	74	66	68	91	103	89	62	56	154	–	–	41	–	–
Monthly average (μg/m ³)																
July	0.56	0.14	0.57	0.21	0.10	0.22	0.43	0.03	0.05	0.79	0.02	1.95	4.07	21.8	0.26	0.38
August	0.29	0.07	0.34	0.17	0.08	0.30	0.33	0.02	0.05	0.36	0.04	–	–	14.9	0.26	0.58
September	0.59	0.16	0.46	0.24	0.11	0.34	0.55	0.05	0.05	0.91	0.03	–	–	23.3	0.27	0.42
October	0.46	0.14	0.50	0.25	0.13	0.36	0.65	0.08	0.05	0.70	0.13	2.77	5.10	23.4	0.29	0.54
November	0.33	0.08	0.49	0.33	0.14	0.92	0.76	0.07	0.06	0.51	0.51	2.33	6.81	23.3	0.24	1.00
December	0.32	0.09	0.38	0.44	0.13	1.33	1.41	0.09	0.09	0.70	0.87	2.83	10.4	33.7	0.27	1.39
Warm season average (μg/m ³)	0.48	0.13	0.45	0.21	0.10	0.29	0.43	0.03	0.05	0.69	0.03	–	–	20.0	0.26	0.44
Cold season average (μg/m ³)	0.32	0.08	0.43	0.39	0.13	1.12	1.08	0.08	0.07	0.61	0.69	–	–	28.5	0.25	1.20
C/W	0.7	0.7	0.9	1.9	1.4	3.9	2.5	2.3	1.4	0.9	23	–	–	1.43	1.0	2.7

RSD: relative standard deviation; warm season: includes July, August, September; cold season: includes November and December; C/W: ratio of cold/warm season values.

* EC and OC values available only for July, October, November, and December. “–” data are not available.

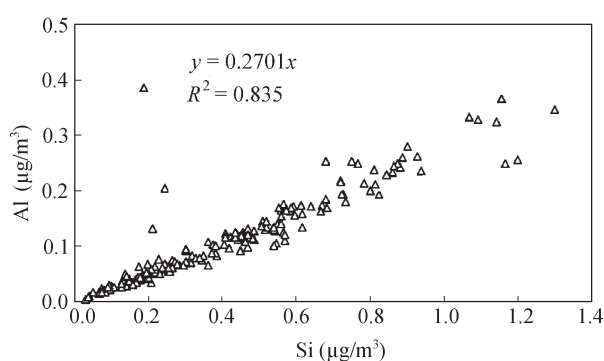


Fig. 1 Plot of Si and Al concentrations from the half year data set from Goess (Styria).

in the current study, that lower concentrations during the cold season (November and December) were caused by occasional snow fall, which suppressed dramatically the abrasion and suspension process. During the dry days in cold season, however, the dust generation process in street may be more effective than that in summer; possibly due to the potential presence of thaw salt and gritting material. The studies on source analysis of PM₁₀ show the elements Ca and Mg to be generated from the street abrasion process or resemble street dust as previous reports (Harrison et al., 2003; Viana et al., 2008). The relationship between Ca and Si during individual days in the Goess data set contrasted with that obtained from Al and Si analyses. There is virtually no correlation between the two elements ($R^2 = -0.150$) as shown in Fig. 2. We hypothesise that mineral material originated directly from street surface abrasion, leading to yield a relatively uniform relationship among Si:Al:Ca, while deviations from this ratio indicate that this resulted from the external influences, e.g., wind did blow directly from other sources, or transferred to the street surface by external sources, and then mobilised by vehicular traffic. A Ca/Si ratio of 0.31 was achieved in the samples collected from a Vienna city highway tunnel emission during weekday and weekend traffic (Handler et al., 2008) as shown in Fig. 2, where the line marked more or less the lower threshold of the Ca/Si relationship. As an

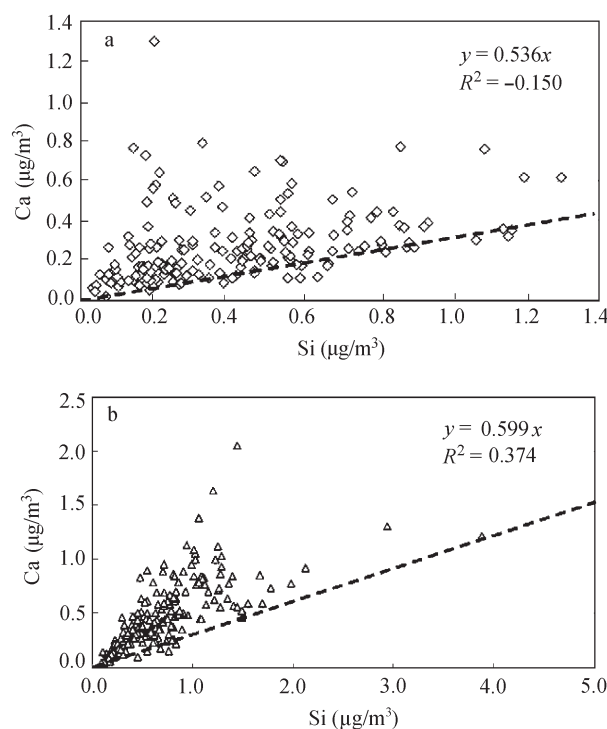


Fig. 2 Plot of Si and Ca concentrations from the half year data set from Goess (Styria) (a) and Donawitz (Styria) (b). The dashed line marks the Ca/Si ratio 0.31 considered the contribution of Ca from street abrasion.

indication, the abrasion of the street surface material was observed also in the Goess region, yielding a Ca/Si ratio of 0.31. In composition with the upper layer of concrete and asphalt surface layers, they varied between regions due to different regional availability of the aggregate material. One possible explanation for a robust correlation of Si and Al and a weak correlation between Si and Ca come from the information from street construction literature, where it is reported, that the uppermost layer of the pavement includes hard and weather durable mineral material (Hunter, 2000). Since silicates are in general harder than calcareous material, we suggest that the correlation between Si and Al reflects the composition of the street surface. The weak correlation with Ca possibly indicates a spurious source

of calcareous material of possibly wind blown. One other possibility is the transport of material from areas where lime and related material are used. Elemental relationships from tunnel samples support these hypotheses (Sternbeck et al., 2002; Hung-Lung et al., 2009).

The Al/Si ratio at the Goess site remained constant with monthly values that were within the range 0.24–0.29 in period July–December (Table 5), which was in close agreement with the ratio 0.28 for literature data for crustal material (Wedepohl, 1995). The Ca/Si ratio, with an average of 0.44 in the “warm season month” (July–September), was higher than that in the street abrasion material (0.31). However, a Ca/Si ratio of 1.2 was significantly greater in the cold season (November and December) and represented a factor of 2.7, which was greater than that in the “warm season”. In the mountainous region of mid Europe, the warm season usually starts at the end of October, following by frost days and snow fall. Since gritting material and thaw salt is used to protect against glazed ice, to increase the grip, and gritting material is frequently of dolomitic nature. In contrast, in the cold season in Austria, thaw salt (NaCl) is used. Consequently, the increase in Ca, Mg, Na and Cl is likely the result of winter services. Based on the Na/Cl stoichiometry, the Na level was a factor of 2 greater than that of NaCl. This data suggested that an additional source of Na was present in the warm season with a concentration of $0.3 \mu\text{g}/\text{m}^3$, while Cl level was very low in the warm season. It is possible that Cl was removed by chemical relaxations that are known to occur under acidic conditions (Hitchcock et al., 1980). It is concluded that the increase in Ca and Mg concentrations in PM_{10} resulted in material applied externally on the road, but it did not originate from direct abrasion of street surface material.

The impact of the biomass combustion smoke on the mineral elements in PM_{10} is due to an increase in K and Zn, and organic carbon as listed in Table 5. This is supported by the evidence as heating was performed at a large fraction by fuel wood combustion (Caseiro et al., 2009) at the forested alpine areas under wintry conditions.

The validity of our hypothesis was tested with the data set of the twin site Donawitz. The absolute values at Donawitz were higher for Si as well as for Ca; however, the lower threshold of the Ca/Si relationship in the graph (Fig. 2b) shows the same slope, as for Goess.

2.2 Warm-cold season differences

According to the short term air quality standard of Europe, a daily average of PM_{10} is $50 \mu\text{g}/\text{m}^3$, not to be exceeded more than 35 times a year at many densely populated sites in Europe (Puteaud et al., 2004). Values exceeding these prescribed levels occur mostly during the cold season, which may be a consequence of conditions of reduced dispersion, compared to warm season. Additionally, we also examined whether the mineral constituents in PM_{10} increase from warm to cold season and the difference between the warm and cold season. As shown in Fig. 3, the monthly averages of mineral concentrations expressed as oxides. Samples were obtained in July compared to that obtained in December at Goess site. While the constituents

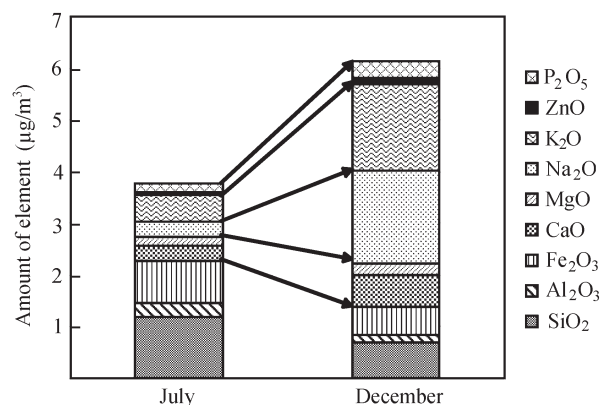


Fig. 3 “Summer” (July)–“Winter” (December) difference at Goess. Elements are expressed as oxides. Major increases originate from Ca, K and Na.

collected mainly from traffic and street abrasion (Si, Al, Fe) show to decrease, Ca, Na, K, Zn and P increase quite notably.

Based on the results from a study of the impact of wood smoke on PM_{10} levels at Austrian sites (Caseiro et al., 2009) and from wood stove combustion tests (Schmidl et al., 2008), it is concluded that the main source for increased K and Zn as well as P values results from wintry domestic wood combustion, while the elevated Ca and Na levels as mentioned earlier are due to winter service for roads, using calcareous gritting and NaCl as thaw salt.

2.3 Weekday-weekend intercomparison

The concentrations of the mineral elements Si, Al, Ca, Mg and Fe are relatively constant throughout the weekdays, but decrease by about 20% to 30% during the weekends, indicating weekday activities—most likely due to reduced heavy traffic and materials handling on weekends (Fig. 4, Table 6). In contrast, the other analytes show no change or increasing concentration on weekends. In the case of K domestic fuel wood combustion is the major influencing factor (Fig. 4). The chloride concentration increased from weekday to weekend is in this case most likely associated with biomass combustion, where Cl/K ratios of 0.1–1 have been observed (Schmidl et al., 2008); while a the general increase in the cold season is linked to thaw salt as well as biomass combustion. Since PM originating from

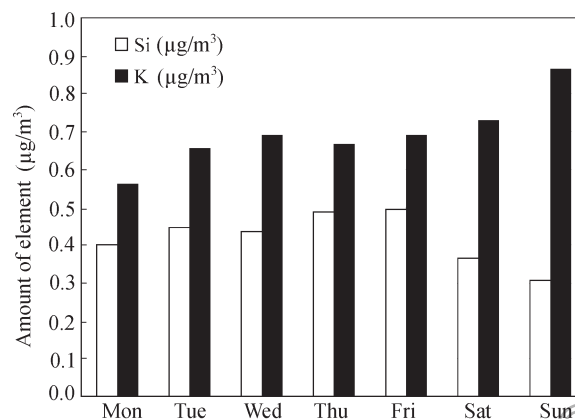


Fig. 4 Averages of the Goess data set for Si and K in a week.

Table 6 Weekday-weekend differences for the half year of Goess data set for mineral elements ($\mu\text{g}/\text{m}^3$)

	Si	K	Fe	Ca	S	P	Al	Mg	Na	Zn	Cl
Monday	0.40	0.56	0.46	0.26	0.59	0.05	0.11	0.11	0.64	0.05	0.27
Tuesday	0.45	0.66	0.52	0.31	0.62	0.05	0.12	0.14	0.59	0.07	0.29
Wednesday	0.44	0.69	0.47	0.29	0.65	0.06	0.11	0.13	0.48	0.05	0.19
Thursday	0.49	0.66	0.52	0.30	0.76	0.06	0.12	0.13	0.55	0.05	0.23
Friday	0.50	0.69	0.45	0.29	0.72	0.06	0.13	0.13	0.60	0.06	0.27
Saturday	0.37	0.73	0.47	0.26	0.66	0.06	0.10	0.09	0.65	0.06	0.33
Sunday	0.31	0.86	0.26	0.22	0.60	0.06	0.09	0.07	0.60	0.05	0.33
Weekday	0.45	0.65	0.48	0.29	0.67	0.06	0.12	0.13	0.57	0.06	0.25
Weekend	0.34	0.79	0.37	0.24	0.63	0.06	0.09	0.08	0.62	0.06	0.33
Weekend/weekday (%)	74	122	76	82	94	106	79	63	109	99	133

thaw salt is expected mainly in the coarse, from biomass combustion, however, in the fine fraction, a discrimination using size fractionating sampling is feasible.

3 Conclusions

The time resolution of 24 hr can be regarded “high” for PM samples for multi element chemical analysis by XRF. The half year data set from Goess site allowed a diagnostic analysis by visual inspection and statistical treatment from the time series plots, and elemental correlations, of weekday-weekend comparison and of the seasonal behavior.

It became evident that the variations of Ca and Mg with time were higher than those of Si and Al. Si and Al were correlated throughout the year. These data suggested a common source of origin, such as abrasion of street surface material. Ca and Mg were, to a small extent, also present in street abrasion material since data from mineral dust analysis in the tunnel study seems to be a strong additional source that increases during the cold season. Compared to July–October, the increase in the November–December points to a specific winter source, which was possibly gritting material from winter services. Gritting materials (mostly dolomite, calcite or less common basalt) are generally used in side streets, while main streets are treated with thaw salt (mostly NaCl). The monthly averages of Si and Al decreased from warm to cold season. Ca, Na and Cl showed a large increase in the cold season. Similarly, Na, K, Zn and P also increased during the cold season. The difference between July and December PM₁₀ is 11.9 $\mu\text{g}/\text{m}^3$. Mineral oxides take part by about 20% of the increase. The main component increasing was organic carbon. Based on the observations of wood smoke, K and the wood smoke tracer levoglucosan (Caseiro et al., 2009) from Austrian sites, we can conclude that the major impact of the winter increase in PM₁₀ at the Goess site originated from wood smoke. The July–December difference in K was approximately 1 $\mu\text{g}/\text{m}^3$ and for OC was 6 $\mu\text{g}/\text{m}^3$. Omitting heteroatoms, the sum of K and OC yields represent 60% of the PM₁₀ increase; assuming a OC-OM conversion factor of 1.3. The sum of K₂O and OM would explain around 75% of the PM₁₀ increase.

The weekday-weekend evaluation indicate a general reduction of between 20% to 30% for the mineral elements Si, Al, Fe, Ca on weekends. Notable increases in K and Cl were interpreted as being a consequence of increasing use

of fuel wood on weekends when families are at home. Cl seems to have originated from thaw salt as well as from biomass combustion, which could be assessed by using size fractionated sampling.

Acknowledgments

The work was in part financed from the projects AQUELLA, AQUELLIS FB and BIOCMB in Austria and the Austrian Exchange Service. It was also supported by the Education Department of Zhejiang Province, China (No. Y200805813). We are grateful to Mr. Hannes Zbiral for his valuable advice regarding XRF analysis.

References

- Bauer H, Marr I, Kasper-Giebl A, Limbeck A, Caseiro A, Handler M et al., 2007. Endbericht für das Projekt “AQUELLA” Wien–Bestimmung von Immissionsbeiträgen in Feinstaubproben. Bericht fr MA22. Vienna University of Technology, Austria.
- Bukowiecki N, Hill M, Gehrig R, Zwicky C N, Lienemann P, Hegedues F et al., 2005. Trace metals in ambient air: hourly size-segregated mass concentrations determined by synchrotron-XRF. *Environmental Science and Technology*, 39: 5754–5762.
- Caseiro A, Bauer H, Schmidl C, Pio C A, Puxbaum H, 2009. Wood burning impact on PM₁₀ in three Austrian regions. *Atmospheric Environment*, 43(13): 2186–2195.
- Gilfrich J V, Burkhalter P G, Birks L S, 1973. X-ray spectrometry for particulate air pollution – A quantitative comparison of techniques. *Analytical Chemistry*, 45: 2002–2009.
- Hammerle R H, Pierson W R, 1975. Sources and elemental composition of aerosol in Pasadena, Calif., by energy-dispersive X-ray fluorescence. *Environmental Science and Technology*, 9: 1058–1068.
- Handler M, Puls C, Zbiral J, Marr I, Puxbaum H, Limbeck A, 2008. Size and composition of particulate emissions from motor vehicles in the Kaisermühlen-Tunnel, Vienna. *Atmospheric Environment*, 42(9): 2173–2186.
- Harrison R M, Jones A M, Lawrence R G, 2003. A pragmatic mass closure model for airborne particulate matter at urban background and roadside sites. *Atmospheric Environment*, 37: 4927–4933.
- Hitchcock D R, Spiller L L, Wilson W E, 1980. Sulfuric acid aerosols and hydrogen chloride release in coastal atmospheres. Evidence of rapid formation of sulfuric acid particulates. *Atmospheric Environment*, 14: 165–182.
- Hung-Lung C, Yao-Sheng H, 2009. Particulate matter emissions from on-road vehicles in a freeway tunnel study. *Atmospheric Environment*, 43(26): 4014–4022.

- Hunter R N, 2000. Asphalts in Road Construction. Telford, London.
- Leland D J, Billbrey D B, Leyden D E, Wobrauschek P, Aiginer H, Puxbaum H, 1987. Analysis of aerosols using total reflection X-ray spectrometry. *Analytical Chemistry*, 59: 1911–1914.
- Limbeck A, Handler M, Puls C, Zbiral J, Bauer H, Puxbaum H, 2009. Impact of mineral components and selected trace metals on ambient PM₁₀ concentrations. *Atmospheric Environment*, 43(3): 530–538.
- Maenhaut W, Cafmeyer J, 1998. Long term atmospheric aerosol study at urban and rural sites in Belgium using multi elemental analysis by particle induced X-ray emission spectrometry and short irradiation instrumental neutron activation analysis. *X-Ray Spectrometry*, 27: 236–246.
- Marcazzan G M, Ceriani M, Valli G, Vecchi R, 2004. Composition, components and sources of fine aerosol fractions using multielemental EDXRF analysis. *X-Ray Spectrometry*, 33: 267–272.
- Merian E, Anke M, Ihnat M, Stoepler M, 2004. Elements and Their Compounds in the Environment. John Wiley & Sons, Weinheim, Germany.
- Puteaud J P, Raes F, Van Dingenen R, Brüeggemann E, Facchini M C, Decesari S et al., 2004. A European aerosol phenomenology-2: Chemical characteristics of particulate matter at kerbside, urban, rural and background sites in Europe. *Atmospheric Environment*, 38: 2579–2595.
- Querol X, Alastuey A, Ruiz C R, Artinano B, Hansson H C, Harrison R M et al., 2004. Speciation and origin of PM₁₀ and PM_{2.5} in selected European cities. *Atmospheric Environment*, 38: 6547–6555.
- Rogge W F, Mazurek M A, Hildemann L M, Cass G R, Simoneit B R T, 1993. Quantification of urban organic aerosols at a molecular level: Identification, abundance and seasonal variation. *Atmospheric Environment*, 27A: 1309–1330.
- Schmidl C, Marr I L, Caseiro A, Kotianová P, Berner A, Bauer H et al., 2008. Chemical characterisation of fine particle emissions from woodstove combustion of common woods growing in mid-European Alpine regions. *Atmospheric Environment*, 42: 126–141.
- Sternbeck J, Sjödin A, Andreasson K, 2002. Metal emissions from road traffic and the influence of resuspension – results from two tunnel studies. *Atmospheric Environment*, 36: 4735–4744.
- Viana M, Kuhlbusch T A J, Querol X, Alastuey A, Harrison R M, Hopke P K et al., 2008. Source apportionment of particulate matter in Europe: A review of methods and results. *Journal of Aerosol Science*, 39: 827–849.
- Wang C F, Chang E E, Chiang P C, 1996. Elemental determination of airborne particulate matter by XRF. *Journal of Radioanalytical and Nuclear Chemistry*, 211: 317–331.
- Watson J G, Chow J C, Frazier C A, 1999. X-ray Fluorescence Analysis of Ambient Air Samples (Landsberger S, Creatchman, eds.). Gordon & Breach, The Netherlands. 67–96.
- Wedepohl K H, 1995. The composition of the continental crust. *Geochimica et Cosmochimica Acta*, 59(7): 1217–1232.